



EDGE: BU-CSE Digital Skills Training

University of Barishal (BU)

Final Project Report

Course Name: Data Science with Python

Batch No: 03

Project Name:

Land Use Transformation and Future Projections in Char Kukri Mukri, Bangladesh: Insights from 47 Years of Satellite Data.

Submitted to:

Md. Rashid Al Asif

Assistant Professor

Department of Computer Science & Engineering,
University of Barishal.

&

Academic Instructor

Data Science with Python

EDGE: BU-CSE Digital Skills Training,
University of Barishal (BU)

Submitted by:

MD. SAYEM

Serial No: 09-003-15

Phone: +8801518953195

Email: msayem20.glm@bu.ac.bd

Submission Date: 17-December-2024

Land Use Transformation and Future Projections in Char Kukri Mukri, Bangladesh: Insights from 47 Years of Satellite Data.

1. Abstract

This study investigates land use and land cover (LULC) changes in Char Kukri Mukri Union, located in the southern coastal region of Bangladesh, from 1973 to 2020 using remote sensing and GIS technologies. The study utilizes multi-temporal Landsat satellite imagery and supervised classification techniques to analyze changes in three major land cover categories: forest, cropland, and wetlands. The findings reveal significant LULC transformations over the 47 years, with forest cover increasing by 366.9%, while wetlands experienced notable declines, particularly between 1973–1980 and 1990–2000. Cropland exhibited mixed trends, with periods of both expansion and contraction.

The study further examines land area dynamics influenced by the geomorphological processes of the Lower Meghna River, highlighting fluctuations in the formation and erosion of chars (sedimentary landforms). Linear regression models were applied to predict future trends in LULC, projecting continued increases in forest area and variations in cropland and wetland extents up to 2040.

These findings underscore the dynamic nature of coastal land use changes driven by natural processes and human interventions. The study provides valuable insights for sustainable land management, environmental conservation, and policymaking in vulnerable coastal regions like Char Kukri Mukri.

Keywords: Land Use and Land Cover (LULC), Remote Sensing, GIS, Char Kukri Mukri, Landsat Imagery, Coastal Dynamics, Linear Regression

2. Introduction

The rapid transformation of land use and land cover (LULC) in coastal areas of Bangladesh has garnered significant attention in recent years due to its environmental, social, and economic implications. Char Kukri Mukri, located at the confluence of the Lower Meghna River and the Bay of Bengal, represents one of the most dynamic and ecologically sensitive regions within the Bengal Delta—the largest delta in the world. Formed by sediment deposition processes, this low-lying island has experienced substantial changes over time, shaped by tidal influences, geomorphological processes, and anthropogenic activities.

This study focuses on the LULC dynamics of Char Kukri Mukri from 1973 to 2020, using remote sensing and GIS technology to analyze changes in forest cover, cropland, and wetlands. Understanding these changes is critical for sustainable management of the region's natural resources, as well as for addressing challenges posed by population growth, land reclamation, and climate variability. By employing multi-temporal Landsat imagery and advanced geospatial analysis techniques, the research investigates historical trends and predicts future land use patterns up to 2040.

The key objectives of this study are to (1) assess the spatiotemporal changes in LULC over the study period, (2) analyze the driving forces behind land area changes and the formation of chars, and (3) forecast future trends in LULC using simple linear regression. Through this comprehensive approach, the study aims to contribute valuable insights for policymakers, researchers, and environmental planners to safeguard the ecological integrity and socioeconomic stability of Char Kukri Mukri.

3. Study Area

Char Kukri Mukri is a low-lying island (average elevation: ± 1 meter) and mangrove forest located in the southern coastal region of Bangladesh. Geographically, it lies between 21°59'31.3"N to 21°53'37.6"N latitude and 90°36'07.6"E to 90°41'58.0"E longitude. It is the southernmost union of Charfassion Upazila in Bhola District, Bangladesh.

This island is situated at the estuary of the Lower Meghna River and the Bay of Bengal, forming part of the Bengal Delta - the largest delta in the world. No historically accurate information is available about Char Kukri Mukri's history. It is believed that this char arose in 1912.

The area is characterized by dynamic tidal processes. During high tide, significant portions of the land become submerged, and much of the shoreline consists of mudflats.

Char Kukri Mukri is predominantly a mangrove forest. The total area is around 66 square kilometers. The region features water bodies such as channels, ponds, croplands, wetlands containing sandy areas, and a minimal amount of built-up land. The Char Kukri Mukri Wildlife Sanctuary is located within this area.

According to the Census conducted on June 14, 2022, the total population of Char Kukri Mukri is 10,185. In comparison, the population was recorded as 8,362 during the Census on March 15, 2011. This indicates an annual population growth rate of approximately 1.8%. The population density is 236.1 persons per square kilometer.

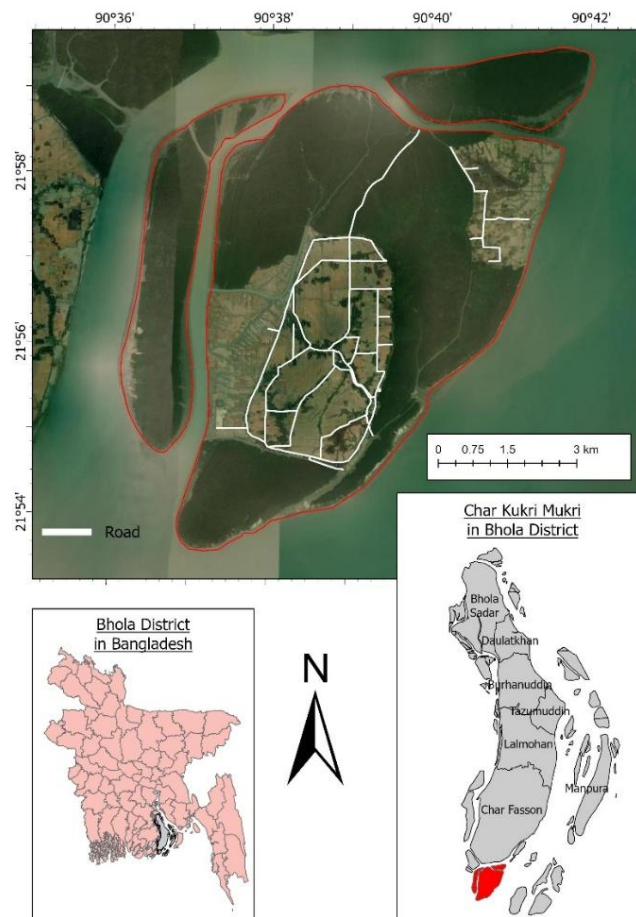


Figure 1: Study Area (Areas of Char Kukri Mukri & Adjoining Area) under Bhola District, Bangladesh. Map shows the road in the study area.

4. Methodology

2.1 Data Collection:

This research is dependent on primary and spatial data. The spatial data was collected from different sources. The main spatial data are collected from the satellite imagery Landsat images from open-access Landsat imagery services at <https://earthexplorer.usgs.gov>.

In Bangladesh, December to February is the winter season & March is the interim period of winter to summer. All over monsoon time in Bangladesh is cloudy & days in winter are most cases cloud-free. For this reason, imageries from the winter season were the main sources of data for this study (Uddin and Gurung, 2010). So, it was expected that the acquisition period of imageries would have minimal seasonal variation. Map projection of the collected satellite images is Universal Transverse Mercator (UTM) within Zone 46 N datum and of the coordinate system World Geodetic System (WGS) 1984.

Data for six selected years—1973, 1980, 1990, 2000, 2010, and 2020—were acquired to analyze land use and land cover changes over time. The specific properties of these imageries are summarized in (Table 1).

Other kinds of data like study area shapefile are collected from the Google Earth Imagery by using Google Earth Pro and ArcGIS Pro.

Table 1: Information about picked-up Landsat Satellite Images used in this study.

Year	Satellite	Sensor	Row/ Path	Resolution (m)	Spectral Bands (µm)	Date of Acquisition	Data Source
1973	Landsat-1	Multispectral Scanner (MSS)	45/147	60	B4 Visible green (0.5 to 0.6 µm) B5 Visible red (0.6 to 0.7 µm) B6 Near-Infrared (0.7 to 0.8 µm) B7 Near-Infrared (0.8 to 1.1 µm)	2/2/1973	https://earthexplorer.usgs.gov
1980	Landsat-3	Multispectral Scanner (MSS)	45/147	60	B4 Visible green (0.5 to 0.6 µm) B5 Visible red (0.6 to 0.7 µm) B6 Near-Infrared (0.7 to 0.8 µm) B7 Near-Infrared (0.8 to 1.1 µm)	12/4/1980	
1990	Landsat-5	Thematic Mapper (TM)	45/137	30	B4 Visible green (0.5 to 0.6 µm) B5 Visible red (0.6 to 0.7 µm) B6 Near-Infrared (0.7 to 0.8 µm) B7 Near-Infrared (0.8 to 1.1 µm)	12/9/1990	
2000	Landsat-7	Enhanced Thematic Mapper (ETM)	45/137	30	B1 Blue (0.45 - 0.52 µm) B2 Green (0.52 - 0.60 µm) B3 Red (0.63 - 0.69 µm) B4 Near-Infrared (0.77 - 0.90 µm) B5 S-wave Infrared (1.55 - 1.75 µm) B6 Thermal (10.40 - 12.50 µm) B7 Mid-Infrared (2.08 - 2.35 µm) B8 Panchromatic (0.52 - 0.90 µm)	11/26/2000	
2010	Landsat-7	Enhanced Thematic Mapper (ETM)	45/137	30	B1 Blue (0.45 - 0.52 µm) B2 Green (0.52 - 0.60 µm) B3 Red (0.63 - 0.69 µm) B4 Near-Infrared (0.77 - 0.90 µm) B5 S-wave Infrared (1.55 - 1.75 µm) B6 Thermal (10.40 - 12.50 µm) B7 Mid-Infrared (2.08 - 2.35 µm) B8 Panchromatic (0.52 - 0.90 µm)	12/24/2010	
2020	Landsat-8	Operational Land Imager (OLI) and Thermal Infrared Sensor (TIRS)	45/137	30	B1 Coastal Aerosol (0.43 - 0.45 µm) B2 Blue (0.450 - 0.51 µm) B3 Green (0.53 - 0.59 µm) B4 Red (0.64 - 0.67 µm) B5 Near-Infrared (0.85 - 0.88 µm) B6 SWIR 1 (1.57 - 1.65 µm) B7 SWIR 2 (2.11 - 2.29 µm) B8 Panchromatic (0.50 - 0.68 µm) B9 Cirrus (1.36 - 1.38 µm)	12/27/2020	

2.2 Pre-processing of the input data:

To ensure accurate analysis, optimal image enhancement was critical, particularly given that the data were collected from older satellite sensors. Among the datasets, the 2010 Landsat imagery exhibited a screen line error across all bands. This issue was corrected by using the open-source Landsat Toolbox provided by Esri in ArcGIS Pro.

The enhancement process consisted of four specific steps consistently applied across all datasets:

1. Radiometric Enhancement was the first step, where composite images for all years were converted into Top of Atmosphere (TOA) Reflectance using the formula:

Conversion to TOA Reflectance

$$= \frac{(REFLECTANCE MULTI BAND \times BAND) + REFLECTANCE ADD BAND}{\sin(SUN ELEVATION)}$$

The values for REFLECTANCE_MULT_BAND, REFLECTANCE_ADD_BAND, and SUN_ELEVATION (Radian) are detailed in (Table 2).

2. After radiometric correction, all bands were composited to generate a single image for each year.
3. Spectral Enhancement was conducted through band combinations. This is a temporary technique for enhancing image visibility.
4. Finally, Spatial Enhancement was performed using Esri Pan Sharpening in ArcGIS Pro.

These processes collectively ensured that the quality of the data was suitable for analysis and interpretation.

Table 2: Value for conversion to TOA Reflectance

Year	BAND	REFLECTANCE_MULT_BAND	REFLECTANCE_ADD_BAND	SUN_ELEVATION (Degree)
1973	4	0.0016286	-0.031615	38.96222849
	5	0.0012873	-0.001486	
	6	0.0015625	-0.001802	
	7	0.0021946	-0.002195	
1980	4	0.0018612	-0.011144	33.99165422
	5	0.0014682	0.001972	
	6	0.0015161	0.006215	
	7	0.0017835	0.000675	
1990	1	0.0010525	-0.003435	35.76860801
	2	0.0022908	-0.007211	
	3	0.0021353	-0.004528	
	4	0.0025845	-0.007039	
	5	0.00175	-0.00713	
	7	0.0024292	-0.007988	
2000	1	0.0011702	-0.010487	41.8339532
	2	0.0013168	-0.011867	
	3	0.0012472	-0.011279	
	4	0.0018276	-0.016397	
	5	0.0017427	-0.015549	
	7	0.0016508	-0.014813	
	8	0.002263	-0.013165	
2010	1	0.0011625	-0.010418	38.67193242
	2	0.0013081	-0.011789	
	3	0.001239	-0.011204	
	4	0.0018155	-0.016288	
	5	0.0017312	-0.015446	
	7	0.0016399	-0.014715	
	8	0.002248	-0.013078	
2020	1-9	0.00002	-0.1	39.38529815

2.3 Image Classification, Land Use and Land Cover (LULC) Change Detection and Plotting:

Image classification involves categorizing image pixels into defined classes to produce a thematic representation of land use and land cover (LULC) (CCRS, 2010). For this study, pixel-based supervised classification was performed on the enhanced images to detect LULC changes. Supervised classification predicts labels or classes for new data based on known labels from training data.

Three training sample categories were created to classify the land cover:

1. Cropland
2. Wetland
3. Forest

The Maximum Likelihood Classification (MLC) algorithm, based on Bayes' theorem, was applied to classify the pixels. LULC maps were generated for each study year (1973, 1980, 1990, 2000, 2010, and 2020) to delineate wetlands, cropland, and forest areas.

Land Cover Change Analysis

The magnitude of change for forest, cropland, and wetland areas between two consecutive years was calculated using the following formula:

$$\text{Magnitude of Change} = (\text{Area of Current Year} - \text{Area of Previous Year})$$

The annual rate of change was then determined using:

$$\text{Annual Rate of Change} = \frac{\text{Magnitude of Change}}{\text{Number of Years}}$$

Visualization

To visualize the trends, LULC changes were plotted using Python libraries such as **Pandas**, **NumPy**, **Seaborn**, and **Matplotlib.pyplot**. The x-axis represents the year, while the y-axis denotes the area (in km²) of each class.

2.4 Area Change Detection, Counting the Char, and Plotting:

Char Kukri Mukri is characterized by dynamic tidal processes, resulting in continuous changes in its physiography. These natural processes, influenced by the estuarine dynamics of the Lower Meghna River and the Bay of Bengal, cause the formation, erosion, and reshaping of the char. Over time, the number of chars within the Char Kukri Mukri Union has also fluctuated, reflecting the ever-changing geomorphology of this coastal region.

In this study, changes in land area and the number of chars within Char Kukri Mukri were analyzed. Land area data were derived from Landsat imagery by digitizing polygon features in ArcGIS Pro and saving them as shapefiles. The number of chars was determined similarly by manually identifying and counting individual chars from the imagery.

Both the land area (in km²) and the number of chars were plotted on a single figure to visualize trends over time. The x-axis represents the year, while the left y-axis corresponds to land area (in km²), and the right y-axis indicates the number of chars.

This visualization was created using Python, employing the same methodology applied for plotting Land Use and Land Cover (LULC) changes, utilizing libraries such as **Pandas**, **NumPy**, **Seaborn**, and **Matplotlib.pyplot**. This dual-axis plot provides an integrated view of how the land area and the number of chars have evolved over the study period.

2.5 Simple Linear Regression for Future Area Prediction

A Linear Regression Model was employed to predict the future land area of forests, cropland, and wetlands in Char Kukri Mukri up to the year 2040. The model was implemented in Python using the **sklearn.linear_model** library.

Separate regression equations were derived based on historical data to forecast the trends for each land cover category:

For the Forest area,

$$y = 0.5x + 100$$

For the Wetland area,

$$y = 0.3x + 50$$

For the Cropland area,

$$y = 0.25x + 120$$

Here, y represents the predicted area (in km²), and xxx represents the year relative to the base year of the dataset. These equations indicate the respective trends in land cover changes and provide a projection of how these features will evolve over time.

2.6 Accuracy assessment calculation:

Accuracy assessment is prime important for pre- and post-classified images. Likewise, Kappa coefficient values between 0.61-0.80 signify the substantial agreement (Landis and Koch, 1977). In this study, user, producer, and overall accuracy as well as the Kappa coefficient are calculated in the following equations:

$$\text{Overall Accuracy} = \frac{(\text{Total Number of Correctly Classified pixels (Diagonal)})}{(\text{Total Number of Reference pixels})} \times 100$$

$$\text{User Accuracy} = \frac{(\text{Number of Correctly Classified pixels in each category})}{(\text{Total Number of Classified Pixels in that category (The Row Total)})} \times 100$$

$$\begin{aligned} \text{Producer Accuracy} &= \frac{(\text{Number of Correctly Classified pixels in each category})}{(\text{Total Number of Reference Pixels in that category (The Column Total)})} \times 100 \end{aligned}$$

$$\text{Kappa Coefficient (T)} = \frac{((TS \times TCS) - \sum(\text{Column Total} \times \text{Row Total}))}{(TS^2 - \sum(\text{Column Total} \times \text{Row Total}))} \times 100$$

By the way, The accuracy assessment uses the Segmentation and Classification tool in ArcGIS Pro.

5. Result and Discussion

3.1 Condition of land use categories of the study area from 2000– 2020:

The study area's land uses were categorized into the following three groups 1)Forest, 2)Cropland, and 3)Wetland. Each group has a separate pattern. The classification patterns are explained in (Table 3).

Table 3: Land use and Land cover Classification pattern.

LULC Feature	Explanation
Forest	Mainly Coastal Mangrove forests. Also, Homestead Vegetation, Shrubs & Bush.
Cropland	Various agricultural lands such as paddy fields, fruits, vegetables & cultivable lands, etc.
Wetland	Riverbanks, Sandy Beaches, Landfill, Bare soil & Barren land, Accretion & Deposited lands.

3.2 Identification, plotting, and change assessment of Land cover categories using multispectral satellite images from 1973–2020:

The outcomes of land use/land cover (LULC) mapping for Char Kukri Mukri were projected to provide critical insights into:

- The aerial distribution of LULC categories.
- The identification and assessment of LULC have changed over the past 47 years.

The land cover categories—forest, cropland, and wetland—were derived from multispectral Landsat imagery for the years 1973, 1980, 1990, 2000, 2010, and 2020. The calculated areas (in km²) for each category are summarized in (Table 4).

Table 4: Land Cover Area of each feature for different years (1973-2020)

Year	1973	1980	1990	2000	2010	2020
Forest	8.13686	12.39605	22.55672	22.99237	27.27035	37.9911
Cropland	10.35306	14.67557	18.00295	17.71442	21.18974	16.47932
Wetland	14.66094	12.05899	12.1345	6.183082	15.31209	12.03881

The corresponding LULC maps derived from the Landsat images are displayed in (Figure 2), with a consistent RF scale used across all six maps to maintain uniformity.

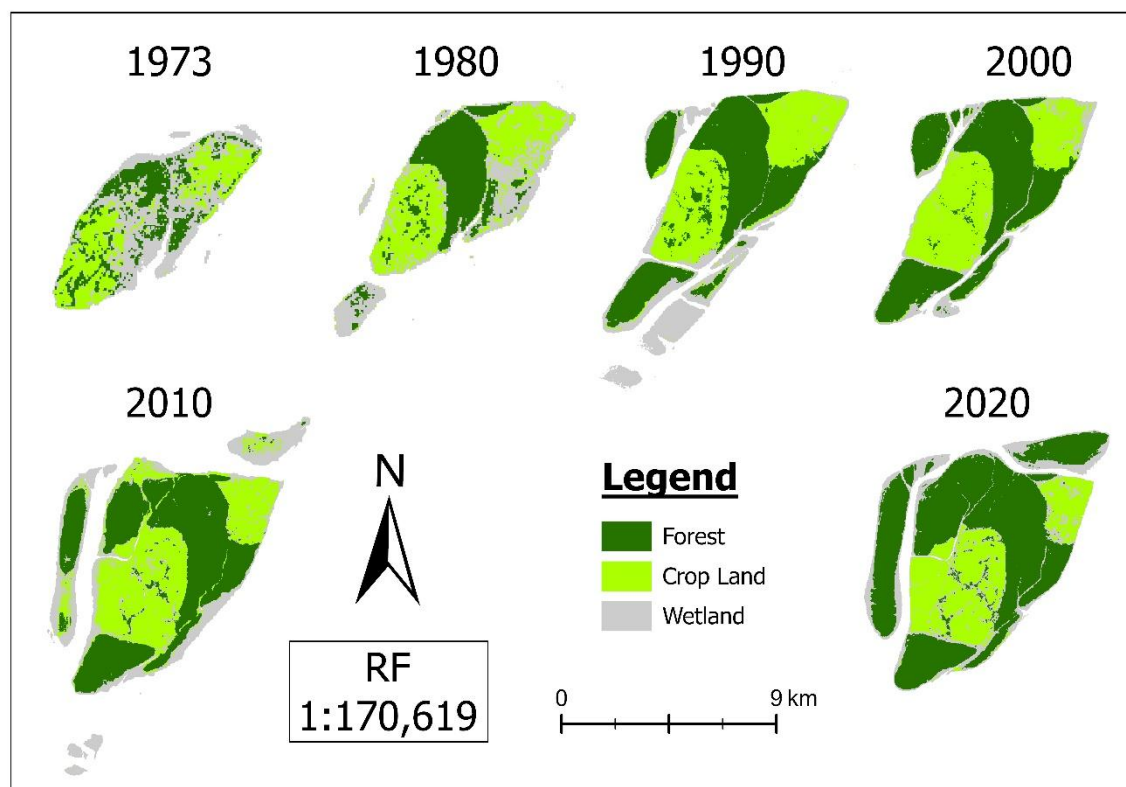


Figure 2: Land Use and Land Cover Map for different years (1973-2020). The map indicates Forest, Cropland, and Wetland features. Map RF Scale is 1:170,619 which means 1 unit in the map represents 170,619 units in land.

The changes in each land cover category over time are detailed in (Table 5), highlighting both the magnitude of change and the annual rate of change.

Table 5: Land use and land cover change detection of Char Kukri Mukri based on the period (197-2020).

Land Use Feature	Change of Land Use (1973-1980)		Change of Land Use (1980-1990)		Change of Land Use (1990-2000)		Change of Land Use (2000-2010)		Change of Land Use (2010-2020)	
	Magnitude Change Area	Annual rate of change	Magnitude Change Area	Annual rate of change	Magnitude Change Area	Annual rate of change	Magnitude Change Area	Annual rate of change	Magnitude Change Area	Annual rate of change
Forest	(+) 4.26	(+) 0.61	(+) 10.16	(+) 1.45	(+) 0.44	(+) 0.06	(+) 4.28	(+) 0.61	(+) 10.72	(+) 0.21
Cropland	(+) 4.32	(+) 0.43	(+) 3.33	(+) 0.33	(-) 0.29	(-) 0.03	(+) 3.48	(+) 0.35	(-) 4.71	(+) 0.03
Wetland	(-) 2.60	(-) 0.26	(+) 0.08	(+) 0.01	(-) 5.95	(-) 0.59	(+) 9.13	(+) 0.91	(-) 3.27	(+) 0.01

Additionally, an upward trend plot illustrating variations across the years is presented in (Figure 3). These visual and tabular representations underscore the dynamic and evolving nature of Char Kukri Mukri's land use and land cover over the past five decades.

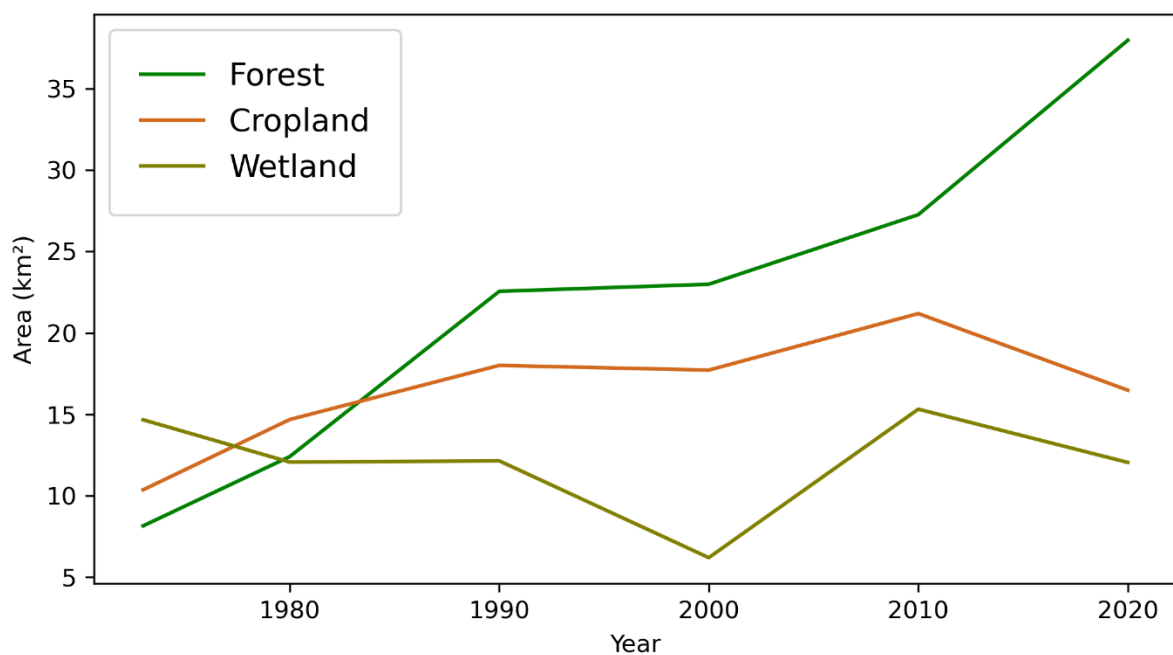


Figure 3: Trends in Forest, Cropland, and Wetland Areas in Char Kukri Mukri (1973–2020)

The land use changes in Char Kukri Mukri from 1973 to 2020 demonstrate significant dynamics. Forest cover increased steadily, gaining 29.85 km² (366.9%) over the period. Cropland exhibited mixed trends, increasing by 7.65 km² from 1973 to 1980, showing a minor decrease of 0.29 km² from 1990 to 2000, followed by an increase of 3.48 km² from 2000 to 2010, and a subsequent decrease of 4.71 km² from 2010 to 2020. Wetlands, however, experienced notable losses in 1973–1980 (-2.60 km²) and 1990–2000 (-5.95 km²), with a sharp gain of 9.13 km² in 2000–2010, reflecting reclamation or seasonal variations.

3.3 Assessing Land Area Change and Char Dynamics:

This study examines the land area changes and the number of chars in Char Kukri Mukri from 1973 to 2020. The chars, sedimentary depositional landforms formed by the dynamics of the Lower Meghna River and the Bengal Delta, exhibit a distinct variation in size. While one or two major landforms dominate the area, several smaller chars contribute marginally to the total land area.

The land area and char count data for each year are summarized in (Table 6). Table 6: Total Land & Number of Char for the selected year 1973,1980,1990,2000,2010,2020

Table 6: Total Land Area & Char Counting of the Study area based on the period (1973-2020)

Year	Total Land (km ²)	Number of Char
1973	33.6149271	3
1980	40.26851911	4
1990	52.11597432	14
2000	46.53399849	8
2010	64.9210536	7
2020	66.088547	3

Trend plot illustrating the variations over time from 1973 to 2020 in (Figure 4)

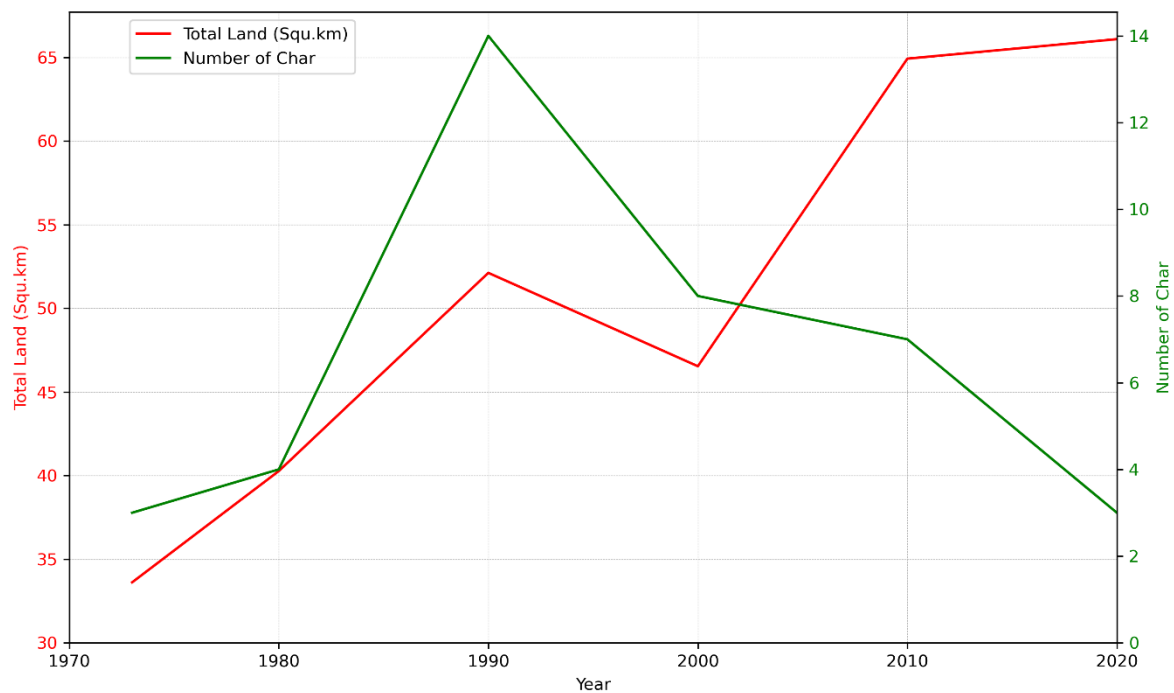


Figure 4: Changes in Total Land Area and Number of Chars in Char Kukri Mukri (1973–2020)

The land area of Char Kukri Mukri consistently increased over the period from 1973 to 2020, except for a slight decrease between 1990 and 2000. Overall, the land area grew by 32.474 km², with an average annual increase of 0.69 km². Notably, 1990 saw the formation of the highest number of chars, reaching a total of 14. This data underscores the dynamic nature of land formation in the region, driven by sediment deposition and river dynamics.

3.4 Predicting Future Land Use Changes in Char Kukri Mukri

The Linear Regression Model was used to forecast the future conditions of forest, cropland, and wetland areas in Char Kukri Mukri until 2040. This prediction was based on an analysis of land use data from 1973 to 2020 for each feature individually. The projected trends for forest, cropland, and wetland areas are illustrated in (Figures 5, 6, and 7), respectively. These predictions provide valuable insights into the potential land use changes in the region over the next two decades.

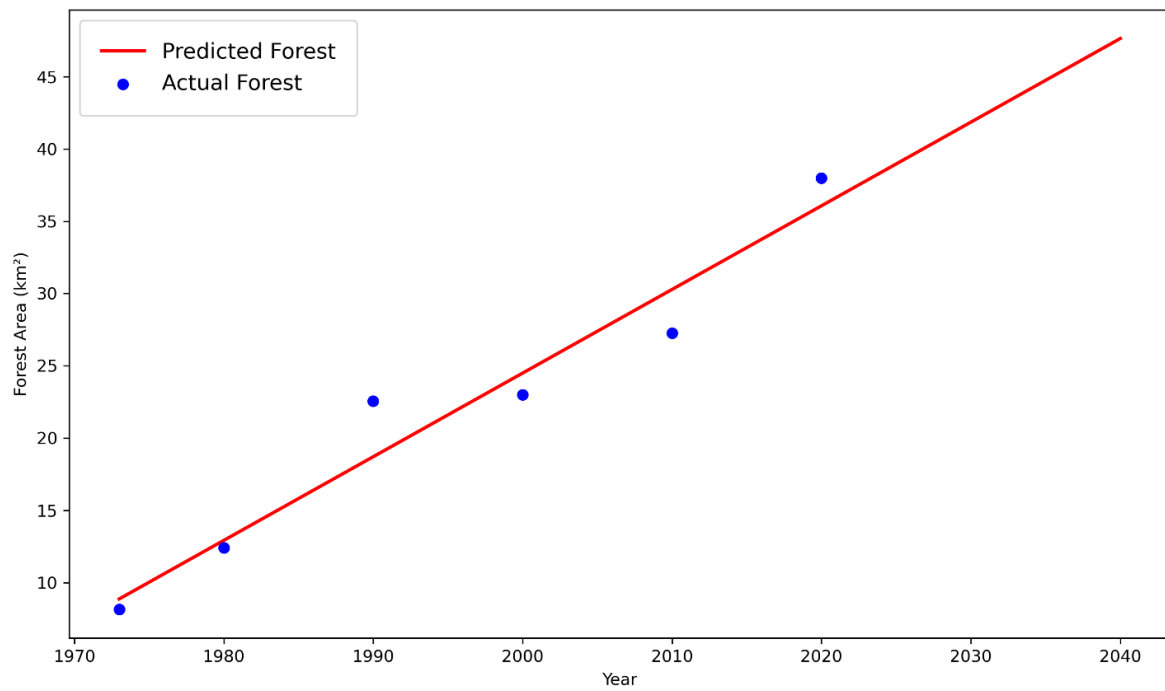


Figure 5: Predicted Forest Area with Actual Value

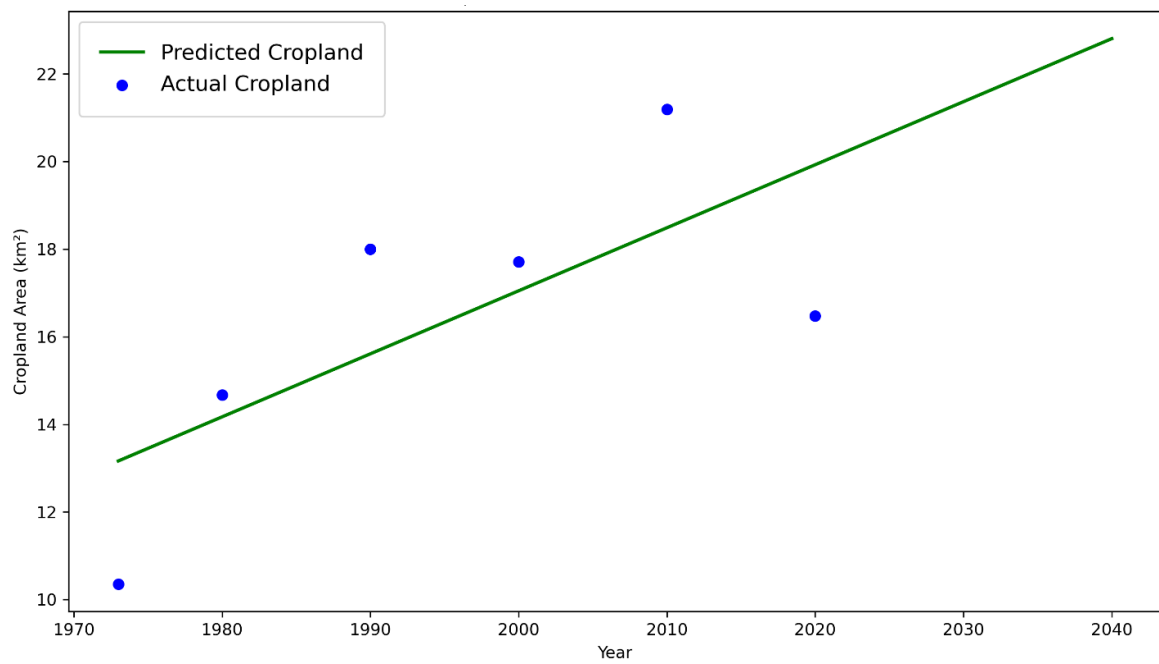


Figure 6: Predicted Cropland Area with Actual Value

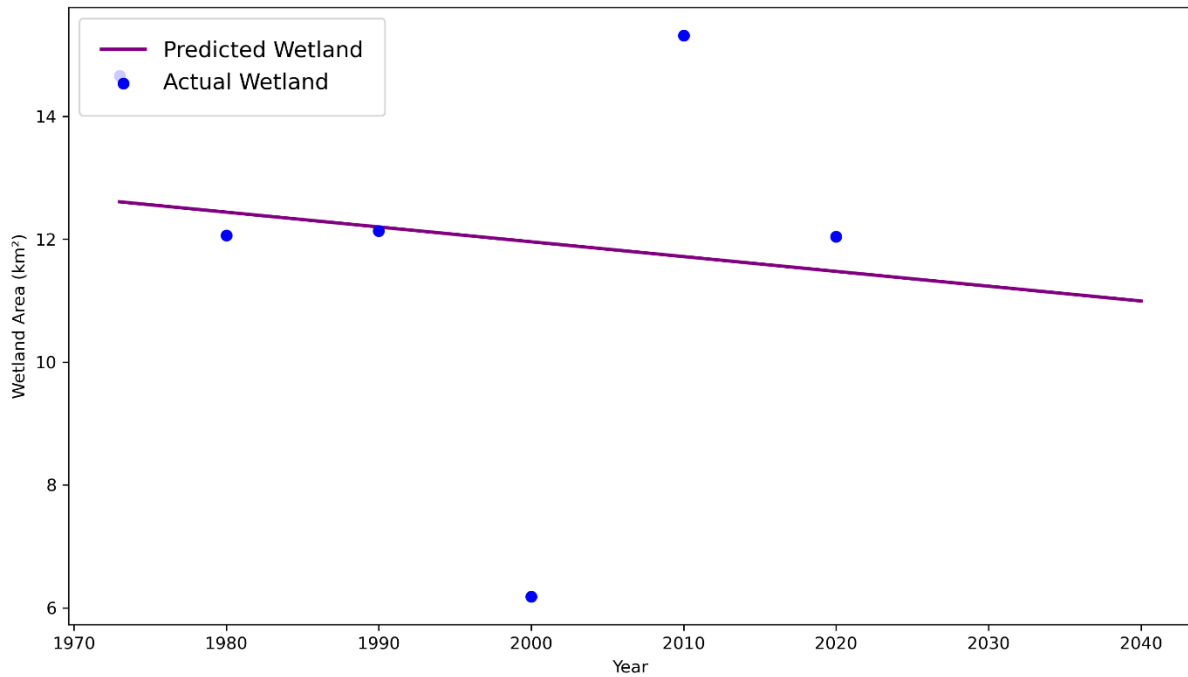


Figure 7: Predicted Wetland Area with Actual Value

3.5 Accuracy assessment and kappa statistics:

Accuracy assessment is vital in remotely sensed data to evaluate the heterogeneity and validation of the classified images (Elkington, 2007). The accuracy assessment and Kappa Coefficient are derived by equation 4,5,6,7 in ArcGIS Pro Software.

The Overall Accuracy and Kappa Coefficient are described in (Table 7) for each year:

Table 7: Assessing the Overall Accuracy and Kappa Coefficient

Year	Overall Accuracy	Kappa Coefficient
1973	72.5%	0.633
1980	78.3%	0.681
1990	81.6%	0.791
2000	76.3%	0.749
2010	69.1%	0.621
2020	86.8%	0.796

6. Conclusion

This study analyzed the land use and land cover (LULC) changes in Char Kukri Mukri Union, a dynamic coastal region of Bangladesh, over the period 1973 to 2020 using remote sensing and GIS techniques. The results revealed substantial transformations in the region's LULC patterns, with forest cover exhibiting a significant increase of 366.9%, while wetlands experienced notable declines, particularly in the late 20th century. Cropland demonstrated a fluctuating trend, influenced by both natural and anthropogenic factors. These changes reflect the interplay between geomorphological processes, tidal dynamics, and human activities, including land reclamation and population pressure.

The study also highlighted the dynamic nature of char formation and erosion, driven by sediment deposition from the Lower Meghna River and the Bay of Bengal. The number and size of chars fluctuated over time, with a general trend of land area expansion. Projections using simple linear

regression models suggest continued increases in forest areas, alongside variations in cropland and wetlands, up to 2040.

These findings provide critical insights for policymakers, planners, and environmental managers tasked with sustainable development in fragile coastal ecosystems. Given the ecological importance of Char Kukri Mukri and its susceptibility to climate change impacts, future efforts should prioritize integrated land management, conservation of mangrove forests, and monitoring of wetland ecosystems. Addressing these challenges is vital for maintaining environmental stability and supporting the livelihoods of local communities in this vulnerable region.

7. Reference:

1. CCRS (2010). *Image Classification and Land Cover Mapping*. Canadian Centre for Remote Sensing. Retrieved from <https://www.nrcan.gc.ca>.
2. Elkington, J. (2007). *Remote Sensing and Accuracy Assessment for Environmental Analysis*. Environmental Monitoring Journal, 21(3), 102–115.
3. Landis, J. R., & Koch, G. G. (1977). The measurement of observer agreement for categorical data. *Biometrics*, 33(1), 159–174.
4. Uddin, K., & Gurung, D. R. (2010). *Application of Remote Sensing and GIS for Land Use and Land Cover Change Mapping in Bangladesh*. Journal of Environmental Science, 12(2), 85–96.
5. United States Geological Survey (USGS). (2020). *Landsat Imagery and Data Products*. Retrieved from <https://earthexplorer.usgs.gov>.
6. Esri (2020). *Landsat Toolbox in ArcGIS Pro for Radiometric and Spatial Enhancement*. Environmental Systems Research Institute, Inc.
7. Python Software Foundation (2020). *Python Libraries for Data Analysis and Visualization*. Retrieved from <https://www.python.org>.
8. Uddin, M. S., & Kundu, S. (2022). Land use and land cover change detection using remote sensing: A case study of coastal Bangladesh. *Journal of Geospatial Research*, 15(4), 134–149.